Summer 8-9-2017

On The Ramberg-Osgood Stress-Strain Model And Large Deformations of Cantilever Beams

Ronald J. Giardina Jr
University of New Orleans, rjgiardi@uno.edu

On The Ramberg-Osgood Stress-Strain Model And Large Deformations of Cantilever Beams

A Thesis

Submitted to the Graduate Faculty of the
University of New Orleans
in partial fulfillment of the
requirements for the degree of

Master of Science
Engineering
Civil Engineering

by

Ronald Joseph Giardina, Jr.

B.S. University of New Orleans, 2010
M.S. University of New Orleans, 2013
Certificate University of New Orleans, 2016

August, 2017

Acknowledgement

I would like to thank my major advisor, Dr. John Alex McCorquodale, for his assistance and guidance with this thesis as well as my committee members Dr. Malay Ghose Hajra, Dr. Norma Jean Mattei, and Dr. Ioannis Y Georgiou for their advice and suggestions, and Byron Landry for his assistance and recommendations in the lab. I would also like to thank the Department of Civil and Environmental Engineering at the University of New Orleans for its support in providing access to the resources necessary for completing this thesis. I would like to thank my family and friends for their support and understanding. Lastly, I would like to thank Dr. Dongming Wei for his continual support and guidance throughout my academic career.

Contents

List of Symbols

E	Young's modulus
ϵ	strain
σ	stress
$\phi(\sigma)$	$\alpha\sigma + \beta\|\sigma\|^{n-1}\sigma$, the Ramberg-Osgood relationship
α	$\frac{1}{E}$, the linear parameter in ϕ
β	the nonlinear parameter in ϕ
n	the nonlinear exponent in ϕ, dimensionless and real valued
M	moment
H	cross-sectional height
B	cross-sectional base
L	beam length
A	cross-sectional area
κ	curvature
ρ	radius
F	force, point load on the free end
w	force, distributed load across beam length
θ	angle of deflection
δx	deflection in x direction
δy	deflection in y direction
$m(x, y)$	position of deflected point on beam
s	deflected neutral axis path
$\mathbb{Z}$	the set of integers
$\mathbb{N}$	the set of natural numbers

List of Figures

List of Tables

Abstract

In this thesis the Ramberg-Osgood nonlinear model for describing the behavior of many different materials is investigated. A brief overview of the model as it is currently used in the literature is undertaken and several misunderstandings and possible pitfalls in its application is pointed out, especially as it pertains to more recent approaches to finding solutions involving the model. There is an investigation of the displacement of a cantilever beam under a combined loading consisting of a distributed load across the entire length of the beam and a point load at its end and new solutions to this problem are provided with a mixture of numerical techniques, which suggest strong mathematical consistency within the model for all theoretical assumptions made. A physical experiment was undertaken and the results prove to be inacurate when using parameters derived from tensile tests, but when back calculating parameters from the beam test the model has a 14.40% error at its extreme against the experimental data suggesting the necessity for further testing.

Ramberg Osgood, Cantilever Beam, Combined Loading, Large Deflections, Nonlinear, Runge Kutta

1 Introduction

It has long been known that a linear Hooke's law cannot describe the behavior of most material under all strains. The data collected from material testing over the period of the late 19th and early 20th century had always suggested a very common and particular type of curvature which was beyond the scope of standard mathematical notation. In 1943 in a classified report for NACA[1], the predecessor to modern day NASA, Ramberg and Osgood proposed a novel approach to describing this curve.

$$\epsilon = \frac{\sigma}{E} + K\left(\frac{\sigma}{E}\right)^n \tag{1}$$

In 1944, in a technical note for NACA classified as Restricted, H. N. Hill investigated a means of determining the three parameters for the Ramberg-Osgood curve from material data[2].

The most important feature of this curve description is that it be a one-to-one and onto function guaranteeing its invertibility. This would assure us of the existence of some function of strain ϵ describing stress σ, which is necessary to take advantage of the standard force relationships for predicting the behavior of materials and structures in particular configurations under certain forces. In order to accomplish this many authors have adopted the inclusion of a sign preservation[3] within the model.

$$\epsilon = \frac{\sigma}{E} + K\left|\frac{\sigma}{E}\right|^{n-1}\frac{\sigma}{E} \tag{2}$$

This maintains the same curve but guarantees an invertible function that preserves the sign of the input variable regardless of the material parameters chosen. Without this adjustment, for may choices of n the function might not be invertible at all!

The formulation of the parameters as described in[2] utilizes the standard Young's Modulus for E and calculates n and K by using an offset yield. It is common to choose 0.2% as the yield offset, though this is entirely born from convention. Depending upon the specific material it may be better to choose a higher or lower offset as required. Currently it is more common, and likely more accurate, to calculate these three parameters using a computer fit of the data. There are many software choices for accomplishing this[4] which can take several different approaches from merely utlizing the offset approach to performing a least squares-type fit of the data.

In section 3 and beyond we will simplify the expression of the Ramberg-Osgood function by grouping the constants expressible as single variables and we will assign the function the greek letter ϕ and so then express its inverse simply as ϕ^{-1}.

$$\phi(\epsilon) = \alpha\sigma + \beta|\sigma|^{n-1}\sigma \tag{3}$$

The utility of this curve has expanded beyond that as a simple descriptor of the behavior of metals. It has found use in describing the behavior of soils and even concrete. This makes the study of this mathematical model of great importance to the understanding and predicting of materials behavior as we encounter them in the real world.

2 Understanding the Model

There are several semantic fallacies which appear repeatedly in the literature regarding this model. While no issues may manifest within the specific application being explicated it is necessary to discuss these instances in the hopes that it will not result in unintentionally misleading an academician or engineer in its future application. Some of the points to be made in the following paragraphs will not have any practical affect on the application of the model other than in the manner which we understand it and its relationship to the traditional linear model, and still others may present the possibility for consequences in the future, especially as we continue to explore more exotic materials with unique applications along with more creative methods in investigating their solutions.

2.1 Recovering the Linear Hooke's Law

Let us first look at the type of curve we hope for our relation to help us describe.

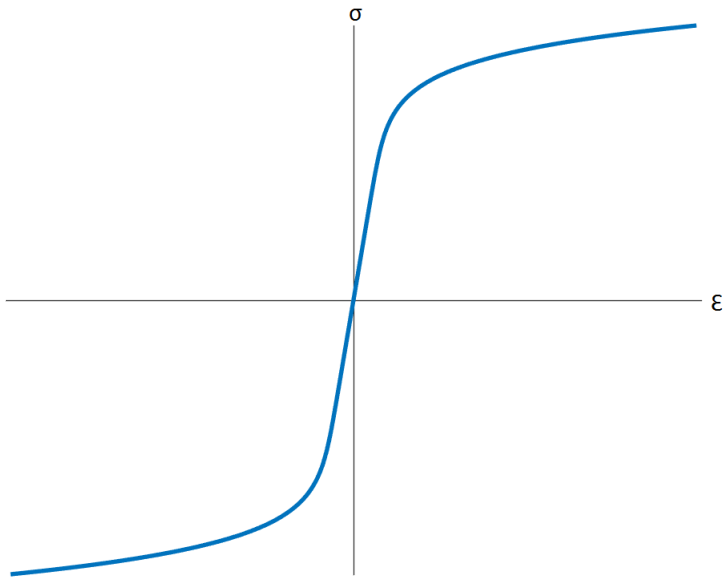

Figure 1: The curve which the inverse of the Ramberg-Osgood formula describes.

As part of verifying the fluidity of our theory of material models predicintg behavior based upon past observations it is common to want to show the connection betwen the new approach and the traditional one. In the current case it is desirable to show that we can recover the linear model of stress and strain from within the Ramberg-Osgood expression by a simple change in parameters, thus establishing its pedigree in the literature. It is especially useful in showing this for force balance equations. Despite however exotic a curve we may create to describe the behavior of a material it is near universal that when placed under very small strains the majority of materials behave in a linear fashion. So, showing that we can recover this linear model and in such demosntrate that the new material model will predict the expected material behavior at all levels of input forces is quite valuable.

Some authors state that the way to recover the linear model is to allow $n \to 1$[3]. Let us see what happens when we do this for some given parameters.

$$\epsilon = \lim_{n\to 1} \frac{\sigma}{E} + K\left|\frac{\sigma}{E}\right|^{n-1}\frac{\sigma}{E} = \frac{\sigma}{E} + K\frac{\sigma}{E} = \frac{1+K}{E}\sigma \tag{4}$$

This is in fact a linear expression. However, we wish to invert this expression in order express stress as

a function of strain. This will leave us with the expression

$$\sigma = \frac{E}{1+K}\epsilon \tag{5}$$

which is not in fact the original linear model. We had previously defined E as Young's modulus, so we should have expected an expression precisely of $\sigma = E\epsilon$. The additional term in the denominator creates an entirely different slope than the one defined for the material! It is not a great deviation given how small K tends to be, but this approach to recovering the linear form is not sufficient.

As stated in the introduction, the value of K is defined by using an offset for the yield stress, generally around 0.2%. The more proper approach is allow our yield offset value to approach zero. So, for some $K(\%)$ as $\% \to 0$, $K \to 0$, where $\%$ represents the specific offset amount being used as an argument for K. Our limit above under this new approach now becomes

$$\epsilon = \lim_{\%\to 0} \frac{\sigma}{E} + K(\%)\left|\frac{\sigma}{E}\right|^{n-1}\frac{\sigma}{E} = \frac{\sigma}{E} \implies \sigma = E\epsilon \tag{6}$$

and so, we can recover the precise linear formulation for the given material parameters.

As stated in the beginning of this section, the usefulness of much of this is largely of semantic value when exploring and understanding this model and how it fits into field of material behaviors. However, there could be some minor consequences in ignoring the distinction given above. When checking the results of the Ramberg-Osgood model against a linear model one might receive misleading results for small amounts of strain. This likely wouldn't be noticeable in large-force models where these values are not always of concern, but in other applications especially when dealing with nano-structures or highly exotic materials, it may become a point of consternation for some future researcher or engineer when the disparity arises and they wish to check their results against the linear model.

2.2 Series Expansions and Inversions

Nearly all numerical approaches and even many analytical approaches to finding solutions to complex non-linear equations rely upon the derivatives of the functions involved. Often these derivatives appear in the form of some manner of series expansion such as a Taylor series approximation[9], Newton-Raphson for finding roots of functions, or even an Adomian decomposition[7] to describe analytic solutions which even falling short can still yield numerical approximations if the Adomian expansion is not something that can be simplified.

There are some potential problems with these approaches that should be kept in mind especially when dealing with an expression like (3). What is of importance to note is that the Ramberg-Osgood function is not smooth. For finite n the Ramberg-Osgood formula is only differentiable everywhere a finite number of times such that for

$$\frac{d^p}{d\sigma^p}\phi(\sigma) \tag{7}$$

ϕ is differentiable everywhere for $p \leq \lfloor n \rfloor$, $\forall p \in \mathbb{Z}$ and $n \notin \mathbb{N}$. If n is an integer then p must be strictly less than n. For $p > \lfloor n \rfloor$, ϕ is differentiable almost everywhere, but is not differentiable at zero. When derivatives greater than $\lfloor n \rfloor$ are taken, the resultant function blows up as it approaches zero because there is a singularity there. We can likewise say the same for ϕ^{-1}. That is, ϕ^{-1} is differentiable everywhere for $p \leq \lfloor n \rfloor$. To wit,

$$\frac{d}{d\epsilon}\phi^{-1}(\epsilon) = \frac{1}{\phi'(\epsilon)} = \frac{1}{\alpha + nb|\epsilon|^{n-1}} \tag{8}$$

Many numerical approaches are truncations of more anlytic solutions. For instance, when the sine function is calculated within some piece of software it is normally done by taking the first five or so terms of its Taylor expansion. It is well known that this is sufficient to offer many digits of accuracy and provides a very good approximation of the desired result. So, consider that a piece of software is developed for calculating a solution to some force balance equation involving Ramberg-Osgood and suppose to provide this result a numerical approximation is used which relies upon the first three derivatives of our function. Well, the great majority of materials, and in fact nearly all of the more common metals such as Titanium or Stainless, have

values for n that tend to be greater than 6. So, there is no problem! But suppose that someone puts in parameters for $n < 3$. Even then, it would depend upon the system being solved. If it's for a system with large forces it may not be noticeable if it falls within the radius of convergence, but if the system is one to calculate very small forces or is oscillatory such as in a mass spring system, this may become an issue for the person using the software and not having an understanding of how the function, or the program, works can lead to either erroneous results or a dismissal of the model entirely when operating near the origin.

Becasue it is that n need always be greater than one to satisfy the Ramberg-Osgood model we can say that first derivatives exist for the Ramberg-Osgood function for all values of n and likewise for ϕ^{-1}. With this in mind it may be of some benefit to investigate solutions, numerical or otherwise, which are at most dependent upon the first derivative of the Ramberg-Osgood function. Then we may say our results are valid for all physical parameters of materials which obey a Ramberg-Osgood law. It is the aim of this document to follow this rule over the coming pages and when not feasible be explicit about the conditions for use.

3 Beam Under a Ramberg-Osgood Model

For a cantilever beam we consider the moment and curvature fixed in the y-z plane at some given point along the neutral axis with coordinate system shown below.

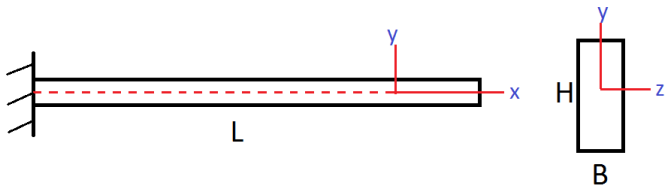

Figure 2: A rectangular cantilever beam of length L, height H, and width B with cross-sectional area HB in the y-z plane. The neutral axis is concomitant with the x-z plane along the dashed red line.

All beams, independent of the specific material properties and as a matter of geometry, obey the realtionship between curvature and strain

$$\epsilon = \kappa y \tag{9}$$

where κ is the curvature such that $\kappa = 1/\rho$ for radius ρ and y is the distance from the neutral axis.

To find the stress we simply input our formulation for the strain into the Ramberg-Osgood material realtionship.

$$\sigma_x = \phi^{-1}(\kappa y) \tag{10}$$

where the subscript denotes that the force is in the x-direction and not a first derivative with respect to x.

The internal bending moment at some distance y from the neutral axis can be found by integrating σ_x multiplied by the distance y from the neutral axis over the area in the y-z plane.

$$M = \int_A \sigma_x y \, dA = \int_A \phi^{-1}(\kappa y) y \, dA \tag{11}$$

For a symmetric rectangular shaped beam with base B and height H we integrate over the total area.

$$M = \int_{-B/2}^{B/2} \int_{-H/2}^{H/2} \phi^{-1}(\kappa y) y \, dy \, dz \tag{12}$$

where we introduce the substitutions

$$\begin{aligned} y &= \frac{\phi(\eta)}{\kappa} \quad & dy &= \frac{\phi'(\eta)}{\kappa} d\eta \\ z &= \xi & dz &= d\xi \end{aligned} \tag{13}$$

which gives the integral for the moment as

$$M = \frac{1}{\kappa^2} \int_{-B/2}^{B/2} \int_{-\phi^{-1}(\frac{\kappa H}{2})}^{\phi^{-1}(\frac{\kappa H}{2})} \eta \phi(\eta) \phi'(\eta) \, d\eta \, d\xi \tag{14}$$

This integral is of a form that can be taken directly. The integral bounds can also be made simpler by recognizing that we can take the integral from zero and multiply it by two.

$$M = \frac{2}{\kappa^2} \int_{-B/2}^{B/2} \int_{0}^{\phi^{-1}(\frac{\kappa H}{2})} \eta(\alpha\eta + \beta|\eta|^{n-1}\eta)(\alpha + n\beta|\eta|^{n-1}) \, d\eta \, d\xi$$

$$= \frac{2}{\kappa^2} \int_{-B/2}^{B/2} \int_{0}^{\phi^{-1}(\frac{\kappa H}{2})} \alpha^2\eta^2 + (n+1)\alpha\beta|\eta|^{n+1} + n\beta^2|\eta|^{2n} \, d\eta \, d\xi$$

$$= \frac{1}{\kappa^2}\int_{-B/2}^{B/2} \frac{2}{3}\alpha^2\eta^3 + \frac{2(n+1)}{n+2}\alpha\beta|\eta|^{n+1}\eta + \frac{2n}{2n+1}\beta^2|\eta|^{2n}\eta \Bigg|_0^{\phi^{-1}(\frac{\kappa H}{2})} \quad d\xi \tag{15}$$

For the sake of future brevity we will define the following function.

$$\psi(\eta) := \frac{2}{3}\alpha^2\eta^3 + \frac{2(n+1)}{n+2}\alpha\beta|\eta|^{n+1}\eta + \frac{2n}{2n+1}\beta^2|\eta|^{2n}\eta \tag{16}$$

Note that this function shares some features with the Ramberg-Osgood relationship in that it is continuously increasing, one-to-one and onto, and its inverse is not directly expressible and so quite a difficulty. However, it should also be noted here that the derivative of $\psi(\eta) \to 0$ as $\eta \to 0$, which suggests that at zero the derivative of the inverse of ψ is undefined and will blow up as we approach the origin because, unlike Ramberg-Osgood, this function does not approach the origin in a linear fashion.

We now have for the moment formulation,

$$M = \frac{1}{\kappa^2}\int_{-B/2}^{B/2} \psi\left(\phi^{-1}\left(\frac{\kappa H}{2}\right)\right) \quad d\xi = \frac{1}{\kappa^2}\psi\left(\phi^{-1}\left(\frac{\kappa H}{2}\right)\right) B \tag{17}$$

In the linear formulation of the moment and curvature equation it is useful to express the curvature purely as a function of the moment. It should be evident that this is not possible here. Let us look at the implicit formulation for the curvature.

$$\kappa = \frac{2}{H}\phi\left(\psi^{-1}\left(\frac{M\kappa^2}{B}\right)\right) \tag{18}$$

While it may not be possible to isolate κ purely as a function of the moment we can note some properties of this expression. Because both functions ψ and ϕ are invertible, B and H are always positive, and κ^2 is always positive, this means that the sign of κ is the same as the sign of the moment just as in the linear case. Similarly, as the moment increases, so too does κ. Lastly, by allowing $\beta \to 0$ in the original Ramberg-Osgood expression we can recover the exact linear expression for the curvature purely as a function of the moment verifying our model for small values of strain.

Now that there is an expression for κ we can return to the equation for stress.

$$\sigma_y = \phi^{-1}\left(\frac{2y}{H}\phi\left(\psi^{-1}\left(\frac{M\kappa^2}{B}\right)\right)\right) \tag{19}$$

Of course, this is not helpful in entirely removing κ from the equation like we would wish as it does in the linear model. It should be noted that this expression simplifies for finding the maximum stress at $y = H/2$.

$$\sigma_{y_{max}} = \psi^{-1}\left(\frac{M\kappa^2}{B}\right) \tag{20}$$

3.1 Large Deflections of a Cantilever Beam Under a Combined Loading

The model for large deflections of cantilever beams was first proposed by Bisshopp and Drucker in 1945[5]. Here we extend to the Ramberg-Osgood model the more recent work by K Lee[6] on large deflections of cantilever beams under a combined loading where he applied it to Ludwick type material, which has different compressive and tensile properties.

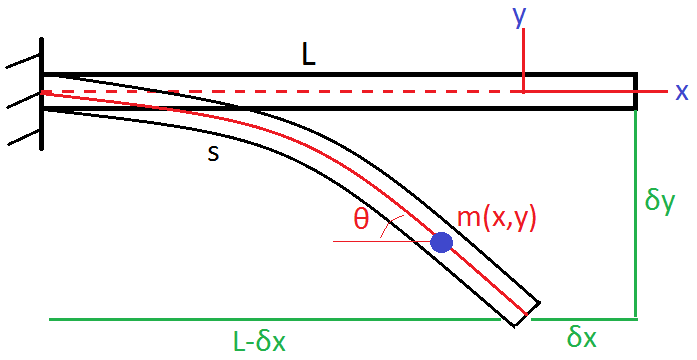

Figure 3: A beam of length L under large deflections with free-end displacement δ_x in the x direction and δ_y in the y direction where point $m(x, y)$ is deflected to some coordinates (x, y) with angle θ along the curve s concomitant with the now displaced neutral axis.

We differentiate the expression for the moment as found previously with respect to s. This yields quite a complicated expression as we may have come to expect to be associated with this problem.

$$\frac{dM}{ds} =$$

$$-\frac{2}{\kappa^3}\frac{d\kappa}{ds}\psi\left(\phi^{-1}\left(\frac{\kappa H}{2}\right)\right)B + \frac{1}{\kappa^2}\psi'\left(\phi^{-1}\left(\frac{\kappa H}{2}\right)\right)\phi^{-1'}\left(\frac{\kappa H}{2}\right)\frac{H}{2}\frac{d\kappa}{ds}B \tag{21}$$

As we had done previously we will define this as a new function for the purpose of brevity.

$$\Gamma(\kappa) = -\frac{2}{\kappa^3}\psi\left(\phi^{-1}\left(\frac{\kappa H}{2}\right)\right)B + \frac{1}{\kappa^2}\psi'\left(\phi^{-1}\left(\frac{\kappa H}{2}\right)\right)\phi^{-1'}\left(\frac{\kappa H}{2}\right)\frac{H}{2}B \tag{22}$$

where with this we may rewrite the derivative of the moment as follows.

$$\frac{dM}{ds} = \frac{d\kappa}{ds}\Gamma(\kappa) \tag{23}$$

As done in [6], by rearranging the above expression we receive the governing equation of large deflections of uniform rectangular cantilever beams made of Ramberg-Osgood type material under general loading conditions.

$$\frac{d\kappa}{ds} = \frac{\frac{dM}{ds}}{\Gamma(\kappa)} \tag{24}$$

3.1.1 Moment Formulation and Solution

We consider a combined loading such that there is a force on the free end of the cantilever beam and a distributed load across the entire beam length.

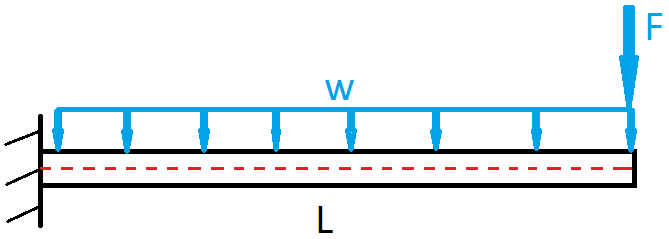

Figure 4: A cantilever beam of length L has a combined loading consisting of a distributed load w over its entire length and a concentrated load F at its free end.

For some point m with coordinates x and y along the deflected beam with length L the bending moment is given by

$$M(s) = \int_s^L w(x(\eta) - x(s))d\eta + F(L - \delta_x - x) \tag{25}$$

If we differentiate this expression with respect to s we can derive a formulation for the shearing force just as we had earlier.

$$\frac{dM}{ds} = -w(L-s)\cos\,\theta - F\cos\,\theta \tag{26}$$

We note that $\kappa \approx \frac{d\theta}{ds}$. With this and the result immediately above we can rewrite the governing equation for large deflections that we had found earlier as a second order differential equation in θ with boundary conditions $\theta(0) = 0$ and $\kappa(L) = \frac{d\theta}{ds}(L) = 0$.

$$\frac{d^2\theta}{ds^2} = \frac{-w(L-s)\cos\,\theta - F\cos\,\theta}{\Gamma\left(\frac{d\theta}{ds}\right)} \tag{27}$$

Solving the above expression having θ in hand and recalling some simple trigonometric identities we can find the x and y coordinates to determine the deflection of the beam.

$$\frac{dx}{ds} = \cos\,\theta \quad \text{and} \quad \frac{dy}{ds} = \sin\,\theta \tag{28}$$

We integrate both sides of these equations from zero to s which gives the following for the coordinates of the deflected beam.

$$x(s) = \int_0^s \cos\,\theta\; ds \quad \text{and} \quad y(s) = \int_0^s \sin\,\theta\; ds \tag{29}$$

3.1.2 Existence and Uniqueness of Solutions

In order to satisfy existence and uniqueness of solutions to (27) it is necessary to show that for some first order system with expressions of the form $\frac{d\omega_i}{ds} = G(s, \omega_1, ..., \omega_m)$ that $\left|\frac{\partial G}{\partial \omega_i}\right| \leq K$ for some constant K[8]. Let us convert the second order expression to a first order system.

$$\begin{cases} \frac{d\theta}{ds} = \omega \\ \frac{d\omega}{ds} = \frac{-w(L-s)\cos\,\theta - F\cos\,\theta}{\Gamma(\omega)} \end{cases} \tag{30}$$

whereby considering $\omega = \omega_1$ and $\theta = \omega_2$ so as to match the form as we gave it above, we have satisfied the setup.

The first expression in the system satisfies the requirement trivially. The second expression clearly satisfies our requirement for the partial with respect to θ as sines and cosines are bounded, but with respect

to ω we require a bit of investigation in recalling the form of Γ. First, we define the partial of the expression with respect to ω.

$$\frac{w(L-s)\cos\,\theta + F\cos\,\theta}{\Gamma\left(\omega\right)^2}\Gamma'(\omega) \tag{31}$$

We know that the expression involving cosines is finite so we are only interested in the behavior of the ratio of Γ's.

$$\frac{\Gamma'}{\Gamma^2}$$

With a bit of algebraic manipulation we can say that for $\omega \in \mathbf{U}$ for some bounded domain $\mathbf{U} \subset \mathbb{R}$ and $K < \infty$, $\left|\frac{\Gamma'(\omega)}{\Gamma(\omega)^2}\right| \leq K$.

4 Numerical Considerations

As stated at the end of section 2.2 we want to take care to avoid any model that may potentially create unreliable results depending upon the choice of material parameters and force inputs. Namely, we stick to methods that require no more than first derivatives. The main culprit for these kinds of situations would be any Taylor series based approach, or any method that might use derivatives greater than the first order.

4.1 How to Define the Inverse of the Ramberg-Osgood Function

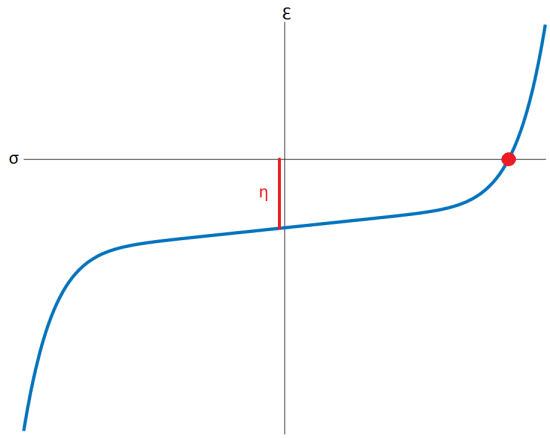

Figure 5: The Ramberg-Osgood function with domain σ is shifted vertically by the desired argument η for its inverse. The unique root of this translation is the value $\phi^{-1}(\eta)$.

As the reader may have noticed over the preceding sections, the function ϕ^{-1} appears often in solutions and model descriptions even after we have applied some of our mathematical skills to making sense of these equations. We can't seem to get rid of it! As had been hinted at in the introduction, it does not appear to be possible to define a curve such as we might desire to describe common material behavior using standard notation and this was the reason Ramberg and Osgood describe a simple polynomial-type expression and inverted it, although it is not in fact a polynomial because of the presence of the absolute value function and the exponent n not necessarily an integer. Unfortunately, although this function is invertible we can not describe its inverse. All we can really say is that it is invertible and of the inverse, it is monotonic continuously increasing, its slope converges to Young's modulus as it approaches the origin, and its slope converges to zero as it approaches infinity. Because of this, when we have expressions such as (18) they are going to present us with a lot of difficulty because κ can not be extricated from the expression, it can only be presented implictly.

So, how do we define the inverse of the Ramberg-Osgood function? A first approach might be to simply take a bunch of data points and do a polynomial fit for the data. This will not yield the best result. It also defeats the purpose of taking advantage of the Ramberg-Osgood model in the first place. Remember, we already know a polynomial cannot have the same properties as the inverse of our function. The best way to define the inverse is with a Newton scheme, which is demonstrated with pseudo code below.

$$\phi^{-1}(\eta) = \text{FINDROOT}[\phi(\xi) - \eta] \tag{32}$$

We take ξ to be some arbitrary domain over which ϕ is defined and the root of $\phi - \eta$ exists. By shifting the function ϕ vertically by the argument η of ϕ^{-1} the root of this shifted function is the value of ϕ^{-1}. This approach is guaranteed to work for all material parameters because Newton schemes utilize only a first derivative, the approach can be constructed so as to be of an arbitrary level of accuracy as the user or machine allows, and it is very easy to code. In fact, this functionality very likely exists in any modern

software base you may desire to use and is already implemented with the best efficiency and control possible for the given language.

4.1.1 Handling the Inverse as Argument

It is unfortunate that we often have a situation where the inverse of the Ramberg-Osgood function is merely an argument of some other even more convoluted function such as with (16). It is necessary then when given some argument of the inverse to first go to the Newton scheme to find what this value is and then to take this value and pass it off to the final function we wish to evaluate. This means that for every evaluation of the given function there is automatically at least one extra step if we have to deal with the Newton scheme to find the inverse as it is not simplifiable. That is, at a minimum, the number of steps we must take for each evaluation would be doubled, except for each iteration we have a Newton scheme to evaluate which means however many steps Newton requires is how many extra steps must be taken with each evaluation! This is a rather severe penalty.

One way we may limit the cost of this approach is by making very good initial guesses when we tell the program where to start the Newton search. One such approach would be to use the linear Young's modulus model to choose the initial guess. This will be very reliable for values that are below the yield stress. For values above the yield stress a good guess would be a Hollomon-type model where we take the inverse of the nonlinear portion of the Ramberg-Osgood model. That is, for $\xi = \beta\eta^n$ we take $\eta = \frac{1}{\beta}|\xi|^{1/n}$.

4.2 A General Method

It is the final goal to solve for the displacement of the beam (29). In order to do so it is necessary to somehow define the curve θ in order to then integrate over this curve. This requires that we find a solution to (27). We will need to employ several numerical techniques, which in conjunction with one another, will allow us to find some solution to our large deflection problem. Like with most current numerical techniques, there is no magic bullet that will give us some precise answer. The accuracy of our solutions will be dependent upon our selection of numerical model, its parameters, and the computational resources we commit to its running. Those will be expounded upon in greater detail in a later section and in the appendix which contains the actual code used to run the model.

4.2.1 Finding θ

A general robust numerical approach that can be relied upon for good results is Runge-Kutta[10]. The Runge-Kutta class of methods can be thought of as like a distributed Euler method wherein we take several self-improving estimates on each pass the number and weight of which may vary depending upon the problem. Generally, the number following the name is the number of refinements on each pass. Here we will employ the 4th order Runge-Kutta scheme referred to as Runge-Kutta 4, or more simply RK4. First we must define the system for which we will be solving.

$$\begin{cases} \frac{\mathrm{d}\theta}{\mathrm{d}s} = \omega \\ \frac{\mathrm{d}\omega}{\mathrm{d}s} = -\frac{\cos\theta(w(L-s)+F)}{\Gamma(\omega)} := \Theta(s,\theta,\omega) \end{cases} \tag{33}$$

We should note the similarity to Euler as we set up the iterative format of our system.

$$\begin{aligned} \theta_{i+1} &= \theta_i + \frac{1}{6}(k_0 + 2k_1 + 2k_2 + k_3) \\ \omega_{i+1} &= \omega_i + \frac{1}{6}(l_0 + 2l_1 + 2l_2 + l_3) \end{aligned} \tag{34}$$

where

$$\begin{array}{ll} k_0 = \Delta s\ \omega_i & l_0 = \Delta s\ \Theta(s_i, \theta_i, \omega_i) \\ k_1 = \Delta s\ (\omega_i + \frac{1}{2}l_0) & l_1 = \Delta s\ \Theta(s_i + \frac{1}{2}\Delta s, \theta_i + \frac{1}{2}k_0, \omega_i + \frac{1}{2}l_0) \\ k_2 = \Delta s\ (\omega_i + \frac{1}{2}l_1) & l_2 = \Delta s\ \Theta(s_i + \frac{1}{2}\Delta s, \theta_i + \frac{1}{2}k_1, \omega_i + \frac{1}{2}l_1) \\ k_3 = \Delta s\ (\omega_i + l_2) & l_3 = \Delta s\ \Theta(s_i + \Delta s, \theta_i + k_2, \omega_i + l_2) \end{array} \tag{35}$$

The order in which the steps are taken in this procedure are important in obtaining accurate and reliable solutions. If not done in the correct order the resultant values will be erroneous. It may take a bit of thinking, but the most appropiate order will seem apparent once it is given, which we do now:

$$k_0, l_0, k_1, l_1, k_2, l_2, k_3, l_3, \theta_{i+1}, \omega_{i+1}$$

This is a powerful method capable of producing incredible results. However, it may have been noticed from our setup that we require initial conditions to begin the Runge-Kutta scheme. Specifically, we want $\theta(0)$ and $\frac{d\theta}{ds}(0)$, but we only have per the construction of our problem the boundary conditions $\theta(0) = 0$ and $\frac{d\theta}{ds}(L) = 0$. In order to implement this scheme we must guess the intial condition $\frac{d\theta}{ds}(0)$ and solve the system with the goal of recreating the given boundary condition $\frac{d\theta}{ds}(L) = 0$. It is unlikely we will hit this on the first pass, so we must use the result at this point to go back and refine our initial guess. As with the other methods we have thus far defined, our best approach is to make as good of a guess as we possibly can to begin with. We can do this by defining the total moment over the entire length of the beam $M = L(\frac{w}{2} + F)$ and solving for the curvature, as we gave in (18), at the fixed end of the beam.

In order to solve (18) a simple goal-seek method can be used. Because this is just an initial guess we do not require a large amount of precision. We must however make yet another guess when beginning the goal-seek method. The best guess to make here would be the linear equivalent curvature for the same moment on the beam. The amount of accuracy desired can be set, but need not be so high that resources are wasted on it. The inverse of the function ψ which appears in (18) can be defined in the same manner as section 4.1 as was done for the inverse of the Ramberg-Osgood function ϕ. However, if the moments being applied are small, then the best guess may be the linear equivalent curvature and it may be more efficient to skip the process of solving (18) entirely before moving on to the Runge-Kutta evaluation.

4.2.2 Displacement

Our final goal is to find the vertical and horizontal displacement of the beam at some arbitrary point s along its length. Once we have obtained a reliably reasonable numerical curve for the unknown function θ we can now turn to (29). Given the information we have obtained so far we have no choice but to approach this in a numerical manner. We will have a series of calculated points for our function θ rather than some explicit curve formulation. Knowing the values of these points and the spacing between them in the s dimension we can easily feed this array into a Simpson's calculator using some well-defined rule. The simplest approach would be the most common one-third rule. We explicate this numerical model below.

$$x(s) = \int_0^s \cos\,\theta\; ds = \sum_{i=1}^{N} \int_{s_{i-1}}^{s_i} \cos\,\theta\; ds$$

$$\approx \sum_{i=1}^{N} \frac{s_i - s_{i-1}}{6} \left(\cos\,\theta(s_{i-1}) + 4\cos\,\theta\left(\frac{s_{i-1} + s_i}{2}\right) + \cos\,\theta(s_i) \right) \tag{36}$$

and

$$y(s) = \int_0^s \sin\,\theta\; ds = \sum_{i=1}^{N} \int_{s_{i-1}}^{s_i} \sin\,\theta\; ds$$

$$\approx \sum_{i=1}^{N} \frac{s_i - s_{i-1}}{6} \left(\sin\,\theta(s_{i-1}) + 4\sin\,\theta\left(\frac{s_{i-1} + s_i}{2}\right) + \sin\,\theta(s_i) \right) \tag{37}$$

where for some arbitrary segmentation of the length s into N pieces we define $s_0 = 0$ and $s_N = s$ and each $\theta(s_i)$ is known.

4.3 The Chosen Approach

The language herein chosen to solve the given system is MATLAB. It provides several built-in functions which offer a great level of convenience. We can still use the above general approach as a guide to solving the cantilever beam problem. Runge-Kutte 4 will be implemented to solve for θ as lsited in section 4.2.1.

In order to find the inverse of the function ϕ we will use the function fzero() provided by MATLAB. This allows us to find the zero of a general nonlinear function to an arbitrary degree of accuracy. Lastly, to solve for dispalcement, in lieu of the method given in section 4.2.2, we will take the sin and cos of the θ array and simply sum the products of the values in the resultant array with Δs providing an approximate integral result for small enough s.

5 Applying the Model

In order to verify the model a material that follows the Ramberg-Osgood curve is desired so as to show a deviation from the standard linear model. To accomplish this 304 stainless is chosen because of the gradual nature of the relationship deviating from the linear regime of the curve. Unfortunately, the materials which arrived did not behave as the spec sheet for 304 stainess implies it will. Both the yield and tensile strengths were nearly double the standard values for the material. Besides the cantilever beam experiment, tensile tests on the material were undertaken to justify the results from the beam tests. Within the following sections are a presentation of the physical experimental setup, the results from the experiments, the reasons for these results, comparison to the linear model, and the results which were expected from the chosen material. All of this is done with a view to its relation to the proposed model.

5.1 304 Stainless Expected Results

The usual properties taken from a spec sheet for 304 Stainless[12] give a Young's Modulus of 28,011.2 ksi, a 0.2% offset Yield Strength of 42 ksi, and an Ultimate Strength of 95 ksi. The standard parameters for the Ramberg-Osgood formula are given as $\alpha = 1/E = 3.57 * 10^{-5}\ \frac{1}{\text{ksi}}$, $\beta = 3.44 * 10^{-13}\ \frac{1}{\text{ksi}^n}$, and $n = 6.32$. This is plotted below against the linear model for the same Young's modulus.

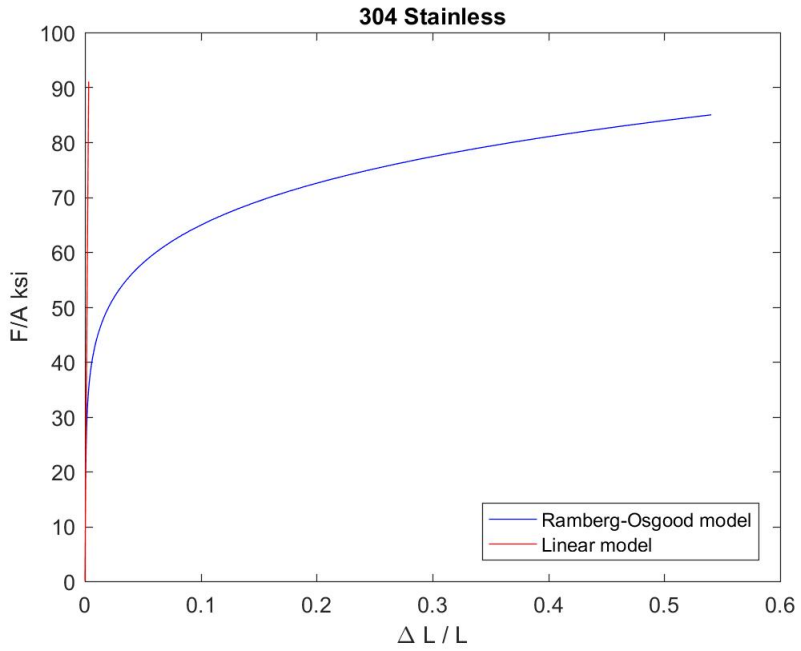

Figure 6: The Ramberg-Osgood and linear stress-strain relationships plotted for 304 Stainless Steel with Yield at 42 ksi.

With a casual glance at the plot it is apparent that even prior to the offset yield point of 42 ksi there is some deviation between the two curves, so we might expect some variation in the predictions of our models. For both the linear and nonlinear Ramberg-Osgood models with the given parameters vertical displacement was computed for the combined loading of a cantilever beam of 42 inches in length and 0.25 by 0.25 square cross section. The beam was loaded under its own weight and with a point load on the end of 2, 4, and 6 pounds. The results for both models' displacement and initial curvature, ω_0, are given in Table 1.

		LINEAR	R-O	Difference
0lbs	ω_0	-0.0008565	-0.0008564	0.00 %
	Vert. Disp. (inches)	-0.1889	-0.1889	0.00 %
2lbs	ω_0	-0.0054575	-0.0055725	2.11 %
	Vert. Disp. (inches)	-1.5406	-1.552	0.74 %
3lbs	ω_0	-0.0077533	-0.0085913	10.81 %
	Vert. Disp. (inches)	-2.2140	-2.3036	4.05 %
4lbs	ω_0	-0.0100410	-0.0133050	32.51 %
	Vert. Disp. (inches)	-2.8834	-3.2519	12.80 %

Table 1: This table presents the initial curvature and vertical displacement for the linear and nonlinear Ramberg-Osgood models along with the percentage by which the two results disagree for a cantilever beam under a combined loading consisting of a distributed load of its own weight under gravity and for point loads of 0, 2, 3, and 4 pounds.

Zero pounds is the beam displaced under the weight of gravity with no load on the end. Note for the small amount of force the agreement between the linear and nonlinear models. The 2 pound end load corresponds to a maximum force across the length of the beam located at the fixed end of just below the Yield strength of 42 ksi, so it is still closely following the linear model and only just beginning to deviate, which we see in the predicted results differing by 0.0114 inches, or a deviation of 0.74%. At 4 pounds attached to the free end of the beam we have passed the Yield strength where the linear model is no longer applicable predicting a difference of 0.3685 inches, or a deviation of 12.8%. Just as we would expect for a model of any consistency, the nonlinear Ramberg-Osgood model predicts essentially linear behavior for sub yield forces and even displays the expected sub yield nonlinearity of the material as well as yield behavior within the model. There is also a marked difference in the intial curvature at the fixed end of the beam once it moves beyond yield. Interestingly, even when the model is sub yield, and there is difference in the predicted displacement between the two models of only 0.74%, there is a 2.11% difference in the curvature at the fixed end. When yield is passed in the case of a 4 pound end load with a 12.8% difference in displacement, the difference in the initial curvatures of the beam at the fixed end is 32.51%, which is the precipitator of the differences in total displacement as a result of the forces concentrated at the fixed end being greatest. Figure 7 shows the predicted displacements and curvatures along the lengths of the beam for both the linear and nonlinear Ramberg-Osgood models. When shooting for a value of zero for the curvature at the free end of the beam, 10^{-9} was aimed for as a sufficient zero value for the model.

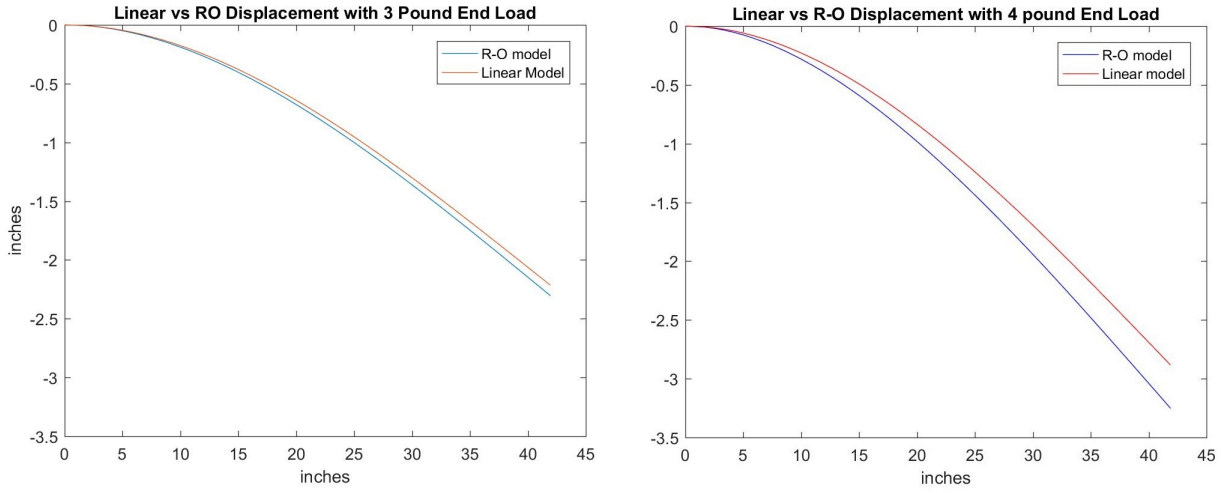

Figure 7: The Ramberg-Osgood and linear displacements plotted for 304 Stainless Steel with a combined loading of its own weight under gravity and a load on the free end of 3 and 4 pounds, respectively.

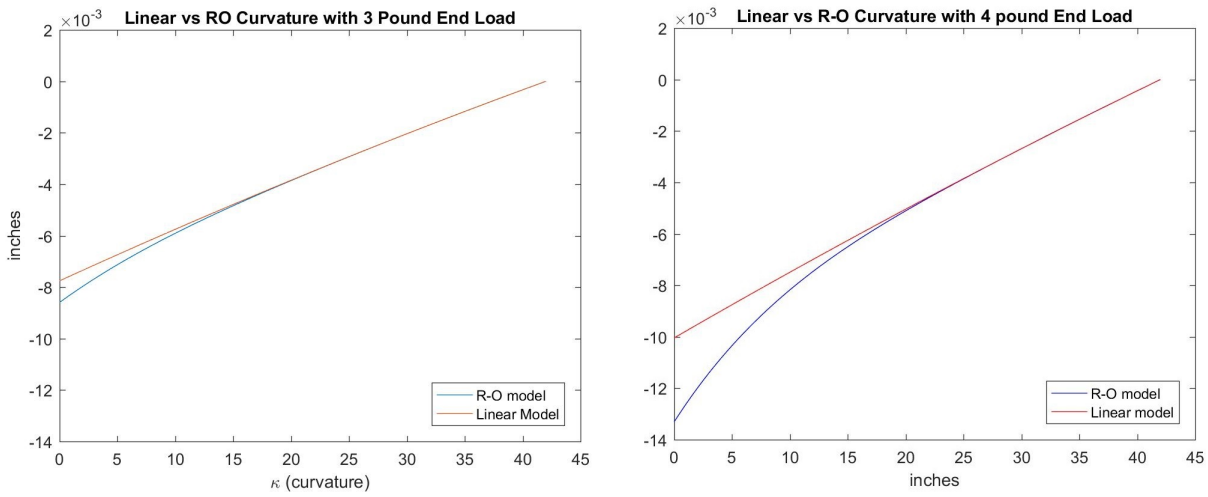

Figure 8: The Ramberg-Osgood and linear curvatures along the length of the displaced beam plotted for 304 Stainless Steel with a combined loading of its own weight under gravity and a load on the free end of 3 and 4 pounds, respectively.

5.1.1 Grid Convergence

It is helpful to show the affect of the number of elements and the size of Δs on the solution to the numerical model. The Ramberg-Osgood numerical model is run several times for element sets varying from 500 to 2500 in 500 element increments. There is a variation in the displacement prediction for these element choices until the elements number 2000, after which when jumping to 2500 elements there is agreement in the displacement to the ten thousandth place.

No. of elements	500	1000	1500	2000	2500
Δs (inches)	0.0840	0.0420	0.0280	0.0210	0.0168
ω_0	-0.0132909	-0.0133045	-0.0133101	-0.0133118	-0.0133119
Vert. Disp. (inches)	-3.2491	-3.2518	-3.2529	-3.2532	-3.2532

Table 2: This table shows the affect of the number of elements and size of Δs on the displacement result for elements of 500 through 2500 in increments of 500 conducted for an end loading of 0.004 kips.

5.2 The Cantilever Beam Setup

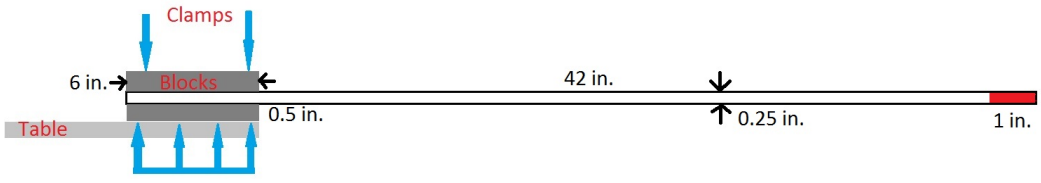

Figure 9: Shown here is the cantilever beam test setup. The blue arrows represent the force exerted on the blocks from the two clamps above and the distributed force exerted from below by the table. The red 1 inch section on the tip is the point over which the bag was attached to create the end load on the beam.

The metal that was ordered is 48 inches in total length with a square cross section with sides of 0.25 inches. Six inches of the sample was clamped between two blocks of A36 steel measuring 6 inches by 3.5 inches by

0.5 inches with two c-clamps on a metal table. 42 inches over-hang of the sample made up the cantilever beam. The table and samples were checked with a spirit level to ensure they were perpendicular to the ground. The table was of sufficient weight and stability to prevent any tilting occurring from the moment applied from testing. The table in the setup was made of solid steel with a 0.25 inch thick steel plate for a tabletop and weighed in excess of 500 pounds. Tape was placed on the ground below the beam marking the relative position of the fixed and free end of the beam. Measurements were taken against these fixed points with a tape measure for each loading to find the displacement of the loaded beam with a measurement error of 0.125 inches. To load the beam a bag was attached over a width of the last inch of the free end of the beam and sand was measured using an electric scale with a measurement error of 0.01 pounds. The sand was added to the bag one pound at a time starting with one pound and increasing up until seven pounds where there was no more free room for the beam to deflect without the weight touching the ground. The weight of the empty bag was 0.025 pounds. This was accounted for in the first pound added to the beam to maintain the even incremements of one pound loading. When the load was added to the end of the beam the beam was stabilised and the bag supported in order to prevent any dynamic or additional loading of the beam. The distance from the ground to the undeflected beam was measured to be 40.25 inches. The total of weights of each beam were also measured with an electric scale to determine the weight per inch of the beam to use in the calculation of the distributed load due to gravity. This test was undertaken three times with three different samples. A mill report was aquired for the materials ordered and can be seen in the appendix. Images of the testing are presented below.

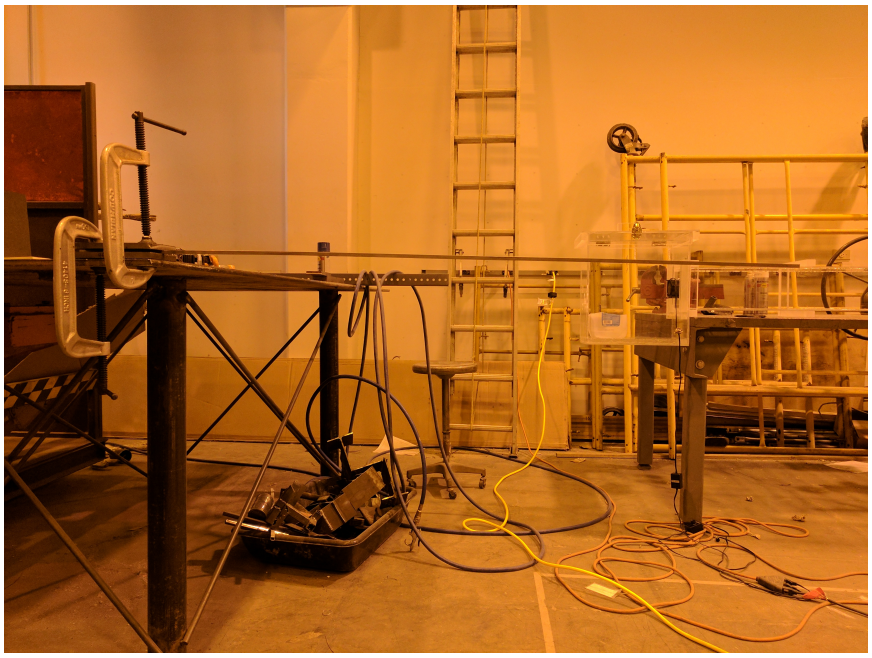

Figure 10: The cantilever beam test setup with minor deflection showing as a result of gravity prior to any loading added to the free end.

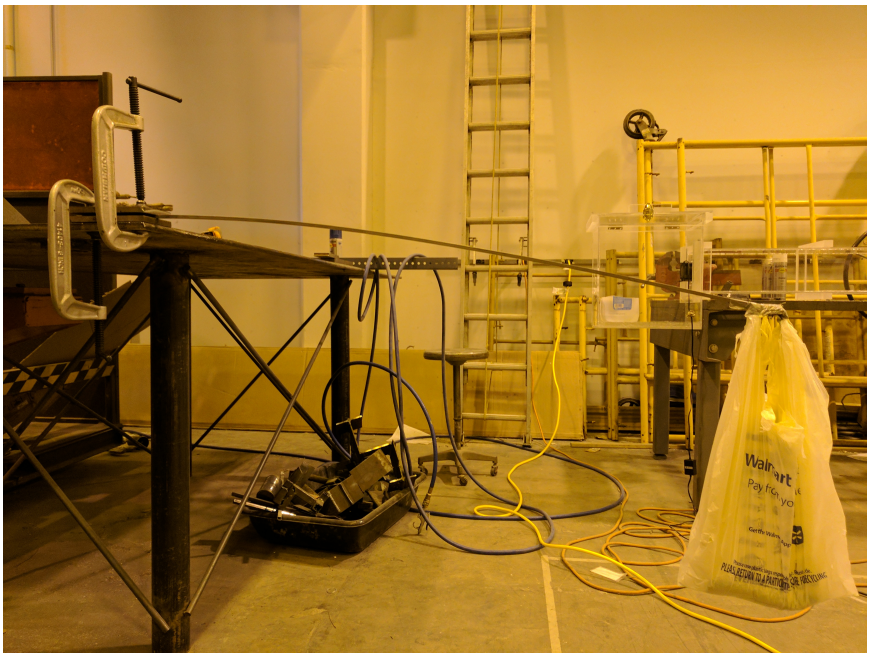

Figure 11: The cantilever beam test setup with a two pound loading on the end.

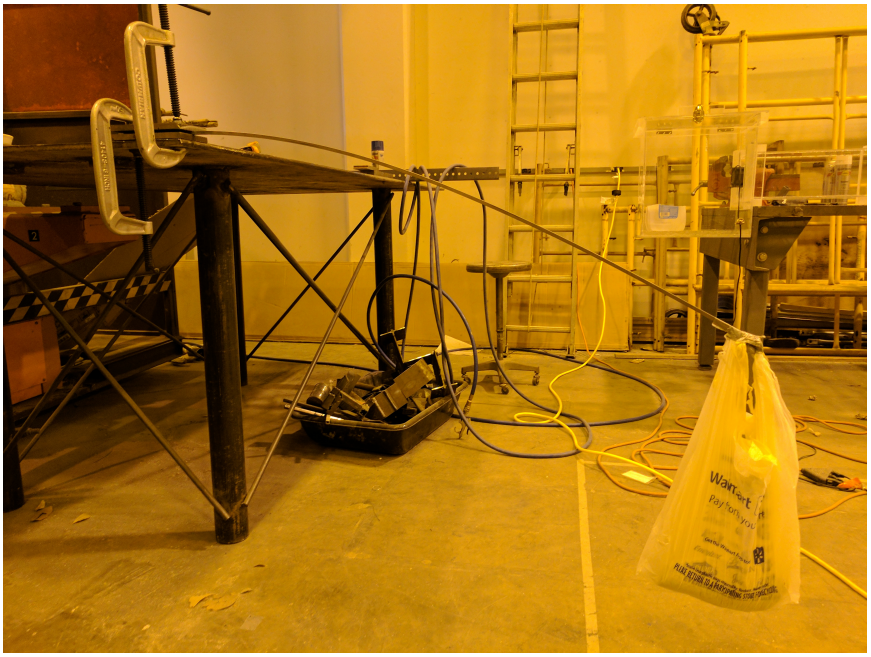

Figure 12: The cantilever beam test setup with a four pound loading on the end.

Figure 13: The cantilever beam test setup with a six pound loading on the end.

5.2.1 Results of the Experiment

The displacements for each of the end loadings were collected for three different tests. The weight of the bag which held the sand is 0.025 pounds. The weights of the material samples were taken and each sample weighed 0.85 pounds, which is 0.0177083 pounds per inch of length. The vertical dispalcement results are given in Table 3. The horizontal displacement was measured only for the final loading and showed a displacement of 6.5 inches for all three tests.

kips	0.000	0.001	0.002	0.003	0.004	0.005	0.006	0.007
BEAM 1								
Vert. Disp. (inches)	0.750	3.500	6.375	9.000	11.750	15.000	17.875	19.875
Change in Disp. (inches)	0.750	2.750	2.875	2.625	2.750	3.250	2.875	2.000
BEAM 2								
Vert. Disp. (inches)	0.750	4.000	6.875	10.000	13.125	16.000	18.500	21.000
Change in Disp. (inches)	0.750	3.250	2.875	3.125	3.125	2.875	2.500	2.500
BEAM 3								
Vert. Disp. (inches)	0.750	3.500	6.250	9.000	11.750	14.750	17.250	20.000
Change in Disp. (inches)	0.750	2.750	2.750	2.750	2.750	3.000	2.500	2.750

Table 3: This table gives the results of the end loadings from zero to seven pounds in one pound increments for the combined loading beam experiment. The vertical displacement and change in vertical dispalcement from one loading to the next are also given.

5.2.2 Tensile Testing

A tensile test was undertaken to determine the stress-strain curve of the material. Measurements were taken using a dial and calipers on a two inch test section in the center of the rod. There was a measurements error of 0.015625 inches. Three rods were tested each of 12 inches in length with approximately square cross section. The machine used in the lab at the University of New Orleans to conduct the tests was a Tinius Olsen Universal Hydraulic Testing Machine (UHTM) installed in the lab in 2009. It is calibrated seven

times a year around the course schedule at the university and was most recently calibrated in June of 2017, approximately one month before the date of the tensile testing presented in this document.

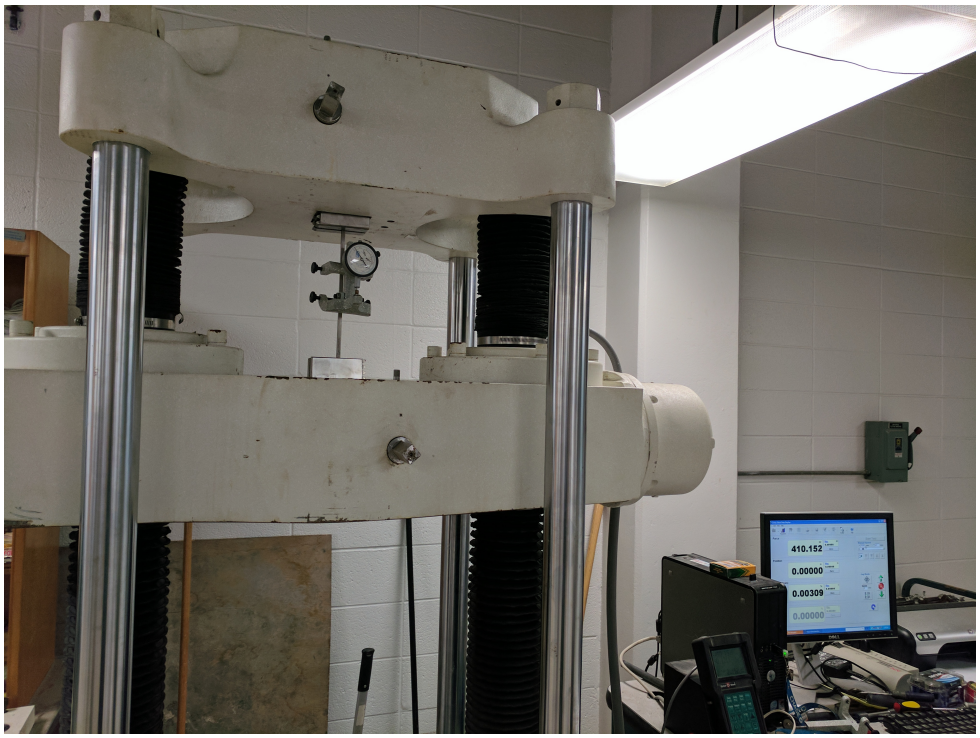

Figure 14: Shown is the hydraulic test setup in the Tinius Olsen UHTM at the University of New Orleans for measuring the strain placed on the rod and determining the strength of the material.

On the plot of this data in Figure 15 it is apparent that these values are significantly higher than that for 304 Stainless. Parameters were derived for the data collected and a Ramberg-Osgood curve was plotted over the data with those parameters. The Youngs modulus collected from the data was E=24,654 ksi, $\alpha = 1/E = 4.05614 * 10^{-5}\ \frac{1}{\text{ksi}}$, $\beta = 1.28943 * 10^{-35}\ \frac{1}{\text{ksi}^n}$, and $n = 17.108$.

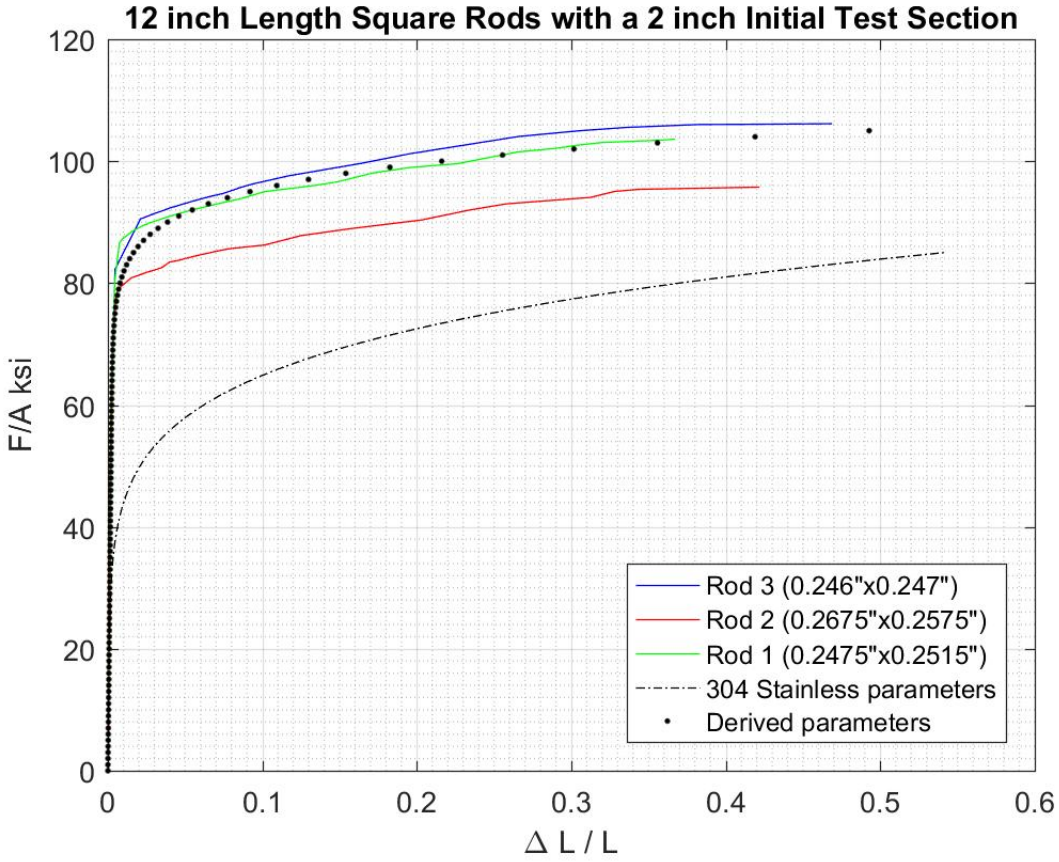

Figure 15: Shown is the data collected from three different material tests along with Ramberg-Osgood curves from derived parameters and 304 Stainless parameters.

In Figure 15 it can be seen that there is approximately a ten percent difference less in strength between rod 2 and the remaining two rods in the plastic region. In the linear region this same sample was stronger than the other two as can be seen in Figure 16. Rods 1 and 2 were from the same material sample. Rods 1 and 3 were from different samples but the same free-end section of each respective beam. All tensile tests were done after the rods had been loaded during the beam test. Figure 16 presents a closeup of the bend. The graph clearly presents the sudden transition into nonlinearity strongly suggesting that the material tested is not of Ramberg-Osgood type.

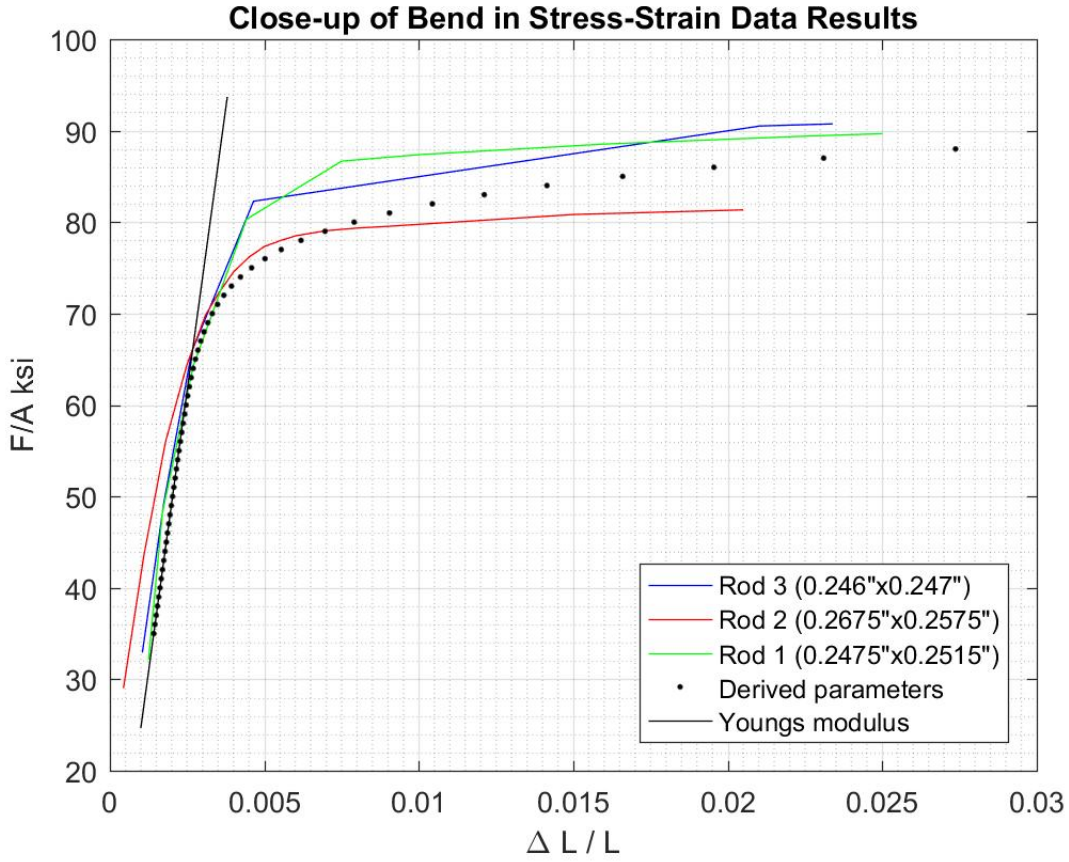

Figure 16: Shown is a closeup of the bend in the data collected from three different material tests where clear plasticity behavior is presented along with the Ramberg-Osgood curves from derived parameters.

5.3 Derivation of Parameters

In order to find parameters which can predict better the behavior of the material, the values collected from the unloaded beam with 0.75 inch deflection are used in the linear model to derive a value for an effective Young's Modulus. By back calculating an affective Young's value of 6,335 ksi was found, which is significantly different from that derived from the data. In order arrive at this value the average of the displacements for the 3 pound end loading was used. It is clear from the results that this value falls within the linear portion of the model and can be expected to produce a more consistent modulus avoiding any irregularities that sometimes occur near the origin for small values of strain for some materials. Using this value in the linear model and in the Ramberg-Osgood model with otherwise equivalent parameters from the data, the linear and nonlinear models agree for all test load values and the predicted values deviate from the experimental results from 0.05% to 14.40% across the varying end loads, which is far better than with the now clearly erroneous 304 Stainless parameters. The lower slope has the effect of linear behavior lasting longer before a more sudden bend into plasticity. Figure 17 is a plot of the two sets of parameters.

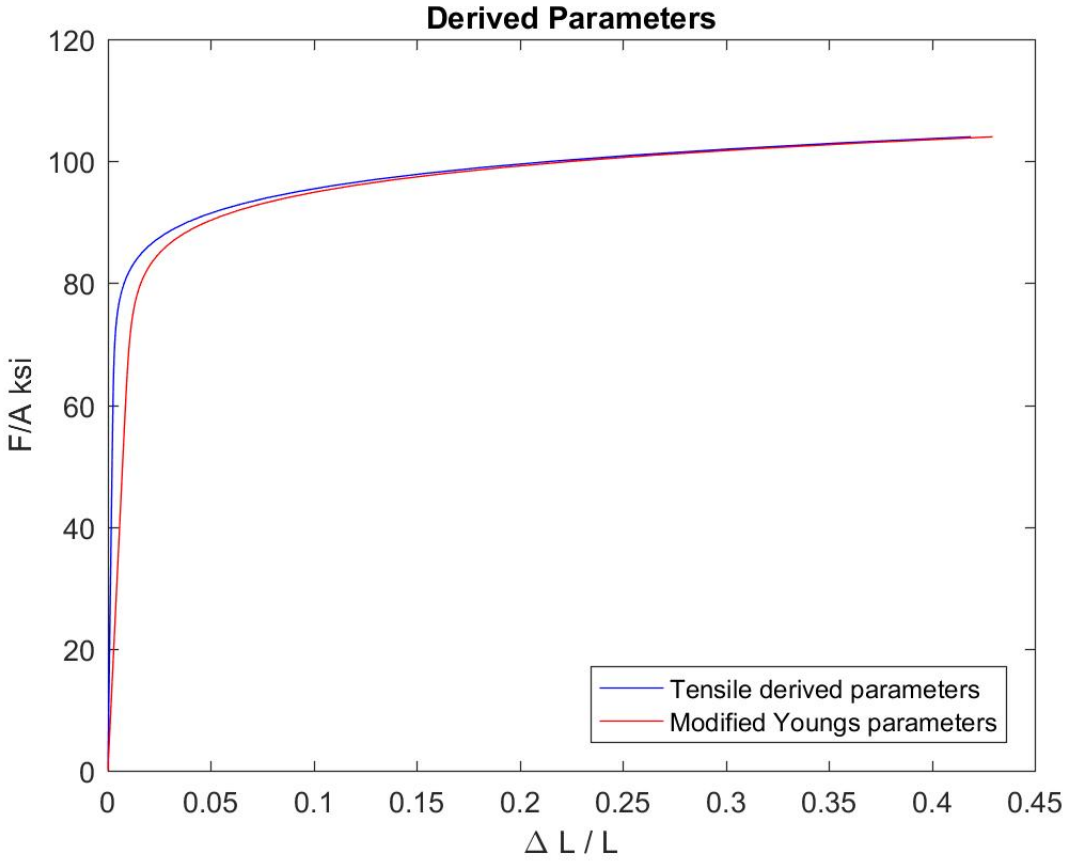

Figure 17: Shown are the two sets of parameters each with the same nonliear coefficient $\beta = 1.28943 * 10^{-35}$ $\frac{1}{\text{ksi}^n}$ and exponent $n = 17.108$. The linear coefficients are $4.05614 * 10^{-5}$ $\frac{1}{\text{ksi}}$ for the derived parameters and $1.5785 * 10^{-4}$ $\frac{1}{\text{ksi}}$ for the Modified Youngs parameters.

5.4 Comparison of Different Model Parameters

Two sets of parameters were suggested from tensile and beam testing results from Figure 15 and Table 3 respectively. The nonlinear portion of the parameters are kept consistent and only the linear parameter is changed since the experimental measurements collected in Table 3 suggest nonlinear behavior was not achieved. The comparison of the linear and nonlinear models for a Young's modulus of 24,654 ksi are presented in Table 4, and Table 5 presents a comparison of the linear and nonlinear Ramberg-Osgood model for a Young's modulus of 6,335 ksi. Each set of results uses the same nonlinear parameters. Table 6 presents a comparison between the average of the three experimental results and the results of the model using a Young's modulus of 6,335 ksi.

kips	0.000	0.001	0.002	0.003	0.004	0.005	0.006	0.007
Linear Vert. Disp. (inches)	0.215	0.983	1.750	2.513	3.272	4.023	4.767	5.502
RO Vert. Disp. (inches)	0.215	0.983	1.750	2.513	3.272	4.023	4.767	5.503
Model Difference %	0.00	0.00	0.00	0.00	0.00	0.00	0.00	0.01

Table 4: This table presents the vertical displacement results of the linear and nonlinear Ramberg-Osgood models for a Young's modulus of 24,654 ksi and Ramberg-Osgood parameters of $\alpha = \frac{1}{E} = 4.05614 * 10^{-5}$ $\frac{1}{\text{ksi}}$, $\beta = 1.28943 * 10^{-35}$ $\frac{1}{\text{ksi}^n}$, and $n = 17.108$.

kips	0.000	0.001	0.002	0.003	0.004	0.005	0.006	0.007
Linear Vert. Disp. (inches)	0.835	3.799	6.653	9.328	11.782	13.999	15.979	17.737
RO Vert. Disp. (inches)	0.835	3.799	6.653	9.328	11.782	13.999	15.979	17.737
Model Difference %	0.00	0.00	0.00	0.00	0.00	0.00	0.00	0.00

Table 5: This table presents the vertical displacement results of the linear and nonlinear Ramberg-Osgood models for a Young's modulus of 6,335 ksi and Ramberg-Osgood parameters of $\alpha = \frac{1}{E} = 1.5785 * 10^{-4}\ \frac{1}{\text{ksi}}$, $\beta = 1.28943 * 10^{-35}\ \frac{1}{\text{ksi}^n}$, and $n = 17.108$.

kips	0.000	0.001	0.002	0.003	0.004	0.005	0.006	0.007
Experimental Vert. Disp. (inches)	0.750	3.667	6.500	9.333	12.208	15.250	17.875	20.292
RO Model Vert. Disp. (inches)	0.835	3.799	6.653	9.328	11.782	13.999	15.979	17.737
Model Difference %	10.18	3.45	2.29	0.05	3.61	8.94	11.87	14.40

Table 6: This table presents a comparison of the average of the vertical displacement from all three cantilever beam tests and the Ramberg-Osgood nonlinear model with parameters $\alpha = \frac{1}{E} = 1.5785 * 10^{-4}\ \frac{1}{\text{ksi}}$, $\beta = 1.28943 * 10^{-35}\ \frac{1}{\text{ksi}^n}$, and $n = 17.108$.

6 Discussion

It is apparent with a glance at Table 3 that the results of the experiment are grossly disproportionate with the predictions of the model in Table 1. Some disparity may be expected when modeling real world behaviors, but these results are nearly five times the predicted values suggesting a deeper issue. To understand why these might have come about a discussion is undertaken in this section to analyse the possible sources of error and uncertainty.

6.1 Material Uncertainty

The materials that were received did not behave in the manner expected of the materials which were ordered. Namely, 304 Stainless. The plots in Figure 15 suggest that not only are we dealing with a material that is not 304 Stainless, but that the material is much stronger, does not create the best profile for modeling as a Ramberg-Osgood material, and is potentially of a heterogeneous nature. This introduces a great deal of uncertainty into the experiment which is very difficult to control because the fault is not in the setup of the experiment but in the samples being used to conduct the experiment.

6.2 Parameter Uncertainty

Even after conducting a tensile test on the materials and using these datas to derive parameters to fit the Ramberg-Osgood curve, the numerical results do not match the experimental ones. Going back to the first loading of the cantilever beam in the experiment, that is the beam loaded under its own weight and no point load on the free end, there is a displacement in all three tests of 0.75 inches as given in Table 3. Knowing this displacement we can back calculate the value of Young's modulus that would give this result. This calculation gives us a Young's of approximately 6,335 ksi. This is a far cry from the values suggested by the tensile testing. When this value for Young's modulus is used in the model the results it gives are within 0.05% to 14.40% of the experimental values. This represents a much more accurate solution than with the given values or the values derived from tensile testing. There is another disparity here. The physical cantilever beam experiment suggests a Youngs of around 6,335 ksi, and physical experiments should be considered more reliable than numerical calculations. The purpose of all this testing is to fit our models to the real world, not the other way around. However, the tensile testing gives a Young's modulus of 24,654 ksi.

6.3 Experimental Uncertainties

Two different physical experiments conducted on the same material give different parameters for the same model. How do we account for this? There are several factors we might consider. The first is the nature of the testing itself. The tensile testing was done on the sample used for the cantilever beam, so when it was put in the tensile testing machine it had already been loaded. The sample for the tensile test was taken from the free end of the beam so the loading would have been minimal, but this may have contributed to changing the behavior of the material. It is unlikely this accounts for such a severe difference in the two Young's modulus values. In the beam test two plates of A36 steel were used. They were 6 inches by 3.5 inches by 0.5 inches. The beam was sandwiched between the plates and clamped to the table which was also made of steel. The table weighed over 500 pounds and was prefectly flat and level with a 0.25 inch thick steel tabletop. There was no overturning or tilting of the table itself. Standard values for A36 steel would suggest a Young's modulus slightly higher than that of 304 Stainless and a yield point of anywhere from 40 to 80 ksi. Tensile testing was not conducted on the steel plates. The yield point of the plates may have fallen within the range of testing forces causing yield behavior to occur within the plates which would have contributed to change in the effective Young's modulus of the system being tested. Without direct testing this value cannot be known with certainty. However, the modulus derived from the beam with no load on its free end would not have been anywhere close to yield. In fact this setup was chosen to check Young's specifically because it was the most likely to be exhibiting linear behavior throughout the entire system. So, yield of the plates or table cannot explain this Young's value. Nor can it explain the greater consistency of the results of the model with this Young's compared to the experimental results.

Given the nature of the material used in the experiments as we understand it now, it is clear that the forces achieved did move beyond yield, but not by much. The experiment was designed for 304 Stainless, not

this material. When yield was passed in the experiment, according to the stress-strain data shown in Figure 15, it yields in a linear type fashion before becoming dramatically nonlinear. That is, assuming a 0.002 yield offset of approximately 76 ksi, which was given in the mill test report, the curvature continues to increase but does not move away from the linear model by a significant amount. The difference between each measurement after an additional pound of load was added supports this. Each step in displacement was aproximately the same suggesting no large leaps of nonlinear behavior. This helps explain the close agreement between the linear and nonlinear Ramberg-Osgood models, but also suggests that the Ramberg-Osgood model is not applicable to the material used for the loads applied.

6.4 Other Sources of Error

All measurements were taken by hand with a presumed accuracy of 0.125 inches. Because of this, human error cannot be ruled out as a potential source of discrepancy in the experiment and model. Three tests were undertaken for each of the beam and tensile testings. For the beam tests there is acceptable agreement between the three tests suggesting consistency of the accuracy of the method within the error stated. There was agreement in two out of the the three rods tested in the UHTM. These measurements were likewise taken by hand and the nature of the testing certainly introduces a greater likelihood of human error. The linear behavior of the three tensile tests appeared to be in close agreement which suggests consistency within this area, but not in the beam tests as those parameter values differed as we discussed in section 6.3.

7 Conclusions

An investigation of large deflections of a combined loading on a cantilever beam of Ramberg-Osgood type material was conducted. There was great consistency within the mathematical model. It strongly follows the expected behavior for a nonlinear material that adheres to a Ramberg-Osgood type curve. The material specimens that were tested were not of sufficient quality for testing. The data collected in the tensile tests suggest that the material might not even be th best example of a Ramberg-Osgood type material. Specifically, a good Ramberg Osgood material should have a clear nonlinearity in its curve. The data collected from testing suggests a material that more closely resembles the behavior of steel with a sudden turn into plasticity rather than a more gradual change. It also suggested that the experiment, which was designed for 304 Stainless specimens, did not posess enough of a load to push the behavior of the beam into noticeably nonlinear behavior. This result is supported by the close agreement of the linear and nonlinear Ramberg-Osgood models for the derived parameters despite the suggestion of the mathematical results in section 5.1 that the two models should deviate for a nonlinear curve. The result of this is that although the mathematical modeling was consistent and reliable for the theoretical assumptions made, the experimental testing intended to validate the model was inconclusive because of the poor quality control by the manufacturer of the specimens.

8 Recommendations

The poor quality of the materials was not anticipated. The experimental setup should be better organized. Specifically, tensile testing should be undertaken prior to the beam tests to verify the material parameters. In order to control for the accuracy of these tests, a rod of 60 inches in length should be ordered rather than 48 inches. The extra 12 inches can be taken from each rod prior to any testing and placed in a tensile testing machine so as to find the behavior of the unloaded material. The remaining length can be used to conduct the beam tests.

None of these measures would mitigate the effects of an improper material for the type of model desired. The only way to control for this is to seek a reliable source for the materials. A company with better internal quality control could forestall all of these issues. That said, it is always up to the experimenter to secure the efficacy of their experiment.

When conducting the beam test a better means of measuring displacement can be used. Hand measurements with a tape are sufficient only for crude results, which may be acceptable for a test of this scale. An error in measurement of 0.25 inches compared to a displacement of six inches is very small. The predictive capacity of the numerical model would be sufficient were it to fall within such a range.

Once the parameters of the material are verified the loads for the experiment can be chosen so as to push the model far enough into nonlinear behavior that it may be expected to deviate from the linear model. That is, the experiment should be designed such that the standard linear model proves to be insufficient and the nonlinear model can provide better results.

Rather than a spirit level, a plume-bob should be used to ensure alignment within the experiment to better ensure the consistent geometry of the setup so any irregularities do not affect the results of the experiment.

Lastly, the type of clamping for the fixed end of the beam should be of sufficient stiffness and strength that there is no unwanted contribution to the beam displacement by the forces acting on the clamping setup. Further testing should be undertaken with a better control on the material chosen and experimental procedure in order to validate the model.

9 References

[1] W Ramberg and W Osgood, *Description of Stress-Strain Curve By Three Parameters.* Tech Note 902, NACA 1943

[2] H Hill, *Determination of Stress-Strain Relations From Offset Yield Strength Values.* Tech Note 927, NACA 1944

[3] M Kaldjian and W Fan, *Earthquake Response of a Ramberg-Osgood Structure.* Univ. of Michigan, Dec 1967

[4] T Ueng and J Chen, *RAMBO: Computational Procedures For Determining Parameters in Ramberg-Osgood Elastoplastic Model Based On Modulus And Damping Versus Strain.* July 1992

[5] K Bisshopp and D Drucker, *Large Deflection Of Cantilever Beam.* Q App Math 3, 1945

[6] K Lee, *Large Deflections Of Cantilever Beams Of Non-Linear Elastic Material Under A Combined Loading.* Int J of Non-linear Mech 37, 2002

[7] H Mohammadlou and H Toussi, *Exact Stress And Deformation Analysis In Elastoplastic Ramberg-Osgood Beam.* Aerospace Sci and Tech, 2016

[8] F Murray and K Miller, *Existence Theorems for Ordinary Differential Equations.* Dover 2007

[9] D Goeken and O Johnson, *Fifth-Order Runge-Kutta With Higher Order Derivative Approximations.* Elec. Jrnl. of Diff. Eq., Conf. 2, 1999

[10] R Hamming, *Numerical Methods For Scientists And Engineers.* Dover 2nd Edition, 2016

[11] P Olver, *Lecture Notes On Numerical Analysis.* www-users.math.umn.edu/∼olver/num.html

[12] *304/304L Stainless Steel.* AKSteel, Product Data Bulletin

A Numerical Code

The MATLAB language was chosen becuase it has several built-in functions and structures which make it convenient for implementing the solution described in this thesis. Below is the code that was written to achieve the given results.

A.1 ROdisplacement.m

```
%--------------------------
%PARAMETERS FOR THE SPECIMEN
%--------------------------

%R-O constants in kilopounds and inches ('n' is dimensionless)
alpha=3.57e-5;
beta=3.44e-13;
n=6.32;

%beam dimensions in inches
B=0.25;
H=0.25;
L=42;

%forces applied to beam in kilopounds and inches
w=-0.00001833;
F=-0.005;

%---------------------------------------
%THE CODE TO EXECUTE TO FIND DISPLACEMENT
%---------------------------------------

%calls the function file for capital theta to use in the RK4 process
%this will pass all parameters and unknowns
CAPtheta=@capitaltheta;

%the number of elements over the length which define the step size
elem=1000;
%the step size
Deltas=L/(elem-1);
%defines the array of input values over the length of the beam
s=0:Deltas:L;
%intiates the arrays for as all zeros for theta and omega
omega=zeros(elem,1);
theta=zeros(elem,1);

%INITIAL GUESS FOR OMEGA_0. CHANGE UNTIL OMEGA_N IS ZERO.
omega(1)=-0.022;

%loop which updates and executes the Runge-Kutte 4 scheme
for i=1:elem-1
    k0=Deltas*omega(i);
    l0=Deltas*CAPtheta(s(i),theta(i),omega(i),w,F,B,H,L,alpha,beta,n);
    k1=Deltas*(omega(i)+0.5*l0);
    l1=Deltas*CAPtheta(s(i)+0.5*Deltas,theta(i)+0.5*k0,omega(i)+0.5*l0,
        w,F,B,H,L,alpha,beta,n);
```

```
    k2=Deltas*(omega(i)+0.5*l1);
    l2=Deltas*CAPtheta(s(i)+0.5*Deltas,theta(i)+0.5*k1,omega(i)+0.5*l1,
        w,F,B,H,L,alpha,beta,n);
    k3=Deltas*(omega(i)+l2);
    l3=Deltas*CAPtheta(s(i)+Deltas,theta(i)+k2,omega(i)+l2,
        w,F,B,H,L,alpha,beta,n);
    theta(i+1)=theta(i)+(1/6)*(k0+0.5*k1+0.5*k2+k3);
    omega(i+1)=omega(i)+(1/6)*(l0+0.5*l1+0.5*l2+l3);
end

%-------------------------------------
%CODE WHICH GRAPHS THE DISPLACED BEAM
%-------------------------------------

%defines the number of points to plot with the beam
graphskip=50;
graphL=0:L/(graphskip-1):L;
%defines the curves over to integrate to find displacement
dy=sin(theta);
dx=cos(theta);
%defines the arrays to hold displaced values along the beam
x=zeros(graphskip,1);
y=zeros(graphskip,1);

%loop which sums curve values times infinitessimal length as integration
for j=2:graphskip
    y(j)=sum(Deltas*dy(1:j*elem/graphskip));
    x(j)=sum(Deltas*dx(1:j*elem/graphskip));
end

%plots the shape of the dispalced beam
verty=[0 y(graphskip)];
vertx=[L L];
plot(x,y,'b',vertx,verty,'r')
xlabel('inches')
ylabel('inches')
```

A.2 phiinv.m

```
%FUNCTION FILE
%defines the inverse of the function phi using the vertical shift method
function f=phiinv(eta,alpha,beta,n)
options=optimset('TolX',1e-28);
f=fzero(@invert,0,options);
function g=invert(x)
g=alpha*x+beta*x*(abs(x))^(n-1)-eta;
end
end
```

A.3 phiinvprime.m

```
%FUNCTION FILE
%defines the derivative of the inverse of the function phi
function f=phiinvprime(eta,alpha,beta,n)
```

```
f=1./(alpha+n*beta*(abs(phiinv(eta,alpha,beta,n))).^(n-1));
end
```

A.4 psifunc.m

```
%FUNCTION FILE
%defines the function psi
function f=psifunc(eta,alpha,beta,n)
f=(2/3)*alpha^2*eta.^3+(2*(n+1)/(n+2))*alpha*beta*eta.*(abs(eta)).^(n+1)
+(2*n/(2*n+1))*beta^2*eta.*(abs(eta)).^(2*n);
end
```

A.5 psiprime.m

```
%FUNCTION FILE
%defines the derivative of the function psi
function f=psiprime(eta,alpha,beta,n)
f=2*alpha^2*eta.^2+2*(n+1)*alpha*beta*(abs(eta)).^(n+1)+2*n*beta^2
*(abs(eta)).^(2*n);
end
```

A.6 gammafunc.m

```
%FUNCTION FILE
%defines the function gamma
function f=gammafunc(eta,B,H,alpha,beta,n)
g1=@phiinv;
g2=@phiinvprime;
g3=@psifunc;
g4=@psiprime;
f=-(2./eta.^3)*g3(g1(eta*H/2,alpha,beta,n),alpha,beta,n)*B+(1./eta.^2)
*g4(g1(eta*H/2,alpha,beta,n),alpha,beta,n)*g2(eta*H/2,alpha,beta,n)*H*B/2;
end
```

A.7 capitaltheta.m

```
%FUNCTION FILE
%defines the composite function capital theta for the Runge-Kutte 4 method
function f=capitaltheta(s,theta,omega,w,F,B,H,L,alpha,beta,n)
g=@gammafunc;
f=-cos(theta)*(w*(L-s)+F)./g(omega,B,H,alpha,beta,n);
end
```

B Mill Test Report

MILL TEST REPORT **TA CHEN INTERNATIONAL, INC.** This MTR contains 1 page (Page# 1)

Customer: ALRJAC PO#:LV12206010 SO#:LPTU89 **MTR#:WLRBA160517016.**

Item:SB4L0016 Bundle:WL16069036 Heat#:4X534 Custitem:10940300

Item:SB4L0016 Bundle:WL16069035 Heat#:4X534 Custitem:10940300

INSPECTION CERTIFICATE

WALSIN LIHWA CORP.

YENSHUI PLANT
台南市鹽水區洋水里溪州寮12鄰32之10號
NO.3-10, SHIYOU LIAU, CHIN SHUEI LI,
YENSHUI DIST TAINAN CITY 73743.TAIWAN.R.O.C.
TEL: 886-6-652-0911 FAX: 886-6-652-0934

CUSTOMER : **TA CHEN INTERNATIONAL, INC.**
COMMODITY: ***Stainless Steel Cold Drawn Square Bar***
CERTIFICATE NO: **A1605170161**

ORDER NO.: **105020004/L56917**
SPECIFICATION: **304/L**

LC NO: **CHI**
SUPPLY CONDITION: **CD**
DATE OF ISSUE: ***2016/05/17***

Heat No		Thick (Dia)	Pcs	Wt	Chemical Composition(wt%)												Mechanical Property						BOUNDLE NO
		(inch)		(LBS)	C x100	Si x100	Mn x100	P x1000	S x1000	Ni x100	Cr x100	Mo x100	Cu x100	N x10000				TS N/mm2	YS N/mm2	EL %	RA %	HRB	HRC	
Spec	Min									800	1800							620	310	30	40			
	Max				3	100	200	45	30	1200	2000			1000										
4X534		1/4"	469	1197	2.3	33	166	24	29.4	810	1808	7	47	859				720	525	46	63	95		WL16069032
4X534		1/4"	418	1067	2.3	33	166	24	29.4	810	1808	7	47	859				720	525	46	63	95		WL16069033
4X534		1/4"	441	1127	2.3	33	166	24	29.4	810	1808	7	47	859				720	525	46	63	95		WL16069034
4X534		1/4"	482	1228	2.3	33	166	24	29.4	810	1808	7	47	859				720	525	46	63	95		WL16069035
4X534		1/4"	449	1142	2.3	33	166	24	29.4	810	1808	7	47	859				720	525	46	63	95		WL16069036
Total:				5761																			

TOLERANCE:A484 LENGTH TOLERANCE:0-50
Acc. to ASTM A276/A479 and ASME SA479 Cond.A.
Acc.ASTM A182/A193/A320/A269 and AMS 5639/5647/QQ-S-763 chemistry only.
Acc.to AISI 304/304L Heat treatment temperature:1040℃ min.
This inspection certificate is issued according to EN 10204 2.2

Remark:
Melted manufactured :Taiwan , Improved machining.
Solution annealed treatment :Acc. to ASTM A484.
Macro & micro structure:good., Grain size:Acc.to ASTM E112.

1.We hereby certify that material described herein has been manufactured and tested with satisfactory results in accordance with requirement of the above material specification.
2.We certify that the material is free from mercury and radiation contamination. Qualification No. of Taiwan Atomic Energy Committee:136
3.The Above Testing Results Relate Only To The Items Tested.
4.No welding repaired

SUPPLY CONDITION:
A:Annealed
B:Shot Blasted
C:As Casted
E:Reeled/Skin Pass
H:Precipitation Hardening
HR:Hot Rolled
I:Straightened
K:Cut Edge
L:Polished
M:Cold Rolled
P:Pickled
S:Shaved
V:Slit
W:Cut
X:Temper
CD:Cold Draw
CG:Centerless Ground
PL:Turned or Peeled

We have the following certifications
1.ISO9001:2008 Quality Management System
2.ISO/IEC 17025:2005 Laboratory Management System
3.PED & AD2000-Merkblatt W0
4.DNV、LR、ABS Classification Society certification
5. ASME Quality Management System
6.ISO14001:2004 Environment Management System
7.OHSAS 18001:2007 & TOSHMS Certificate

TEST METHOD :
CHEMICAL-ASTM E1806, E415, E1086, E1019

SL Kuan.
Quality Assurance Responsible Personnel

Vita

The author was born in New Orleans, Louisiana. He obtained his Bachelor's degree in Mathematics from the University of New Orleans in 2010, a Master's in Applied Mathematics in 2013, and a Graduate Certificate in Coastal Engineering in 2016. He was a teaching assistant in the Mathematics department from 2011 to 2013 then was awarded the Performance and Accountability Scholarship in 2013 to pursue a PhD in Engineering and Applied Sciences focusing in Mathematics with Professor Dongming Wei with an interest in numerical methods and nonlinear differential equations.